argue that the curves (for SIT and saturation) are displaced by a significant amount, however, this displacement is meaningful only if the dipole moment $\wp$ is known. A measurement of the amplitude of the peak of the power spectrum can be used as a direct verification of the area theorem.[1] The spectrum would also help to show whether the carrier could be properly described as a monochromatic wave, or whether there were fast frequency changes present.

We wish to acknowledge helpful and stimulating conversations with Professor E. Hahn and Professor A. Szoke.

PHYSICAL REVIEW B VOLUME 1, NUMBER 1 1 JANUARY 1970

Rotating-Frame Double Resonance and Nuclear Cross Relaxation in LiF†

DAVID V. LANG* AND P. R. MORAN
Department of Physics, University of Wisconsin, Madison, Wisconsin 53606
(Received 4 March 1969; revised manuscript received 8 September 1969)

This paper resports our study of Hartmann and Hahn's technique of rotating-frame nuclear double resonance (RFDR). We consider the Li^6–Li^7 system in LiF and obtain the cross-relaxation dynamics from the Li^7 free-induction-decay data via a general expression which we derive. We find that the presence of F^{19} spins, which constitute a third species interacting strongly with the Li systems in LiF, may easily be taken into account, and that the resulting RFDR behavior does not differ qualitatively from that in a simple two-species system. The cross-relaxation time dependence is well described by an exponential or sum of exponentials for times longer than the order of T_2, with nonexponential behavior for shorter times. The cross-relaxation rate W_{CR} exhibits a Lorentzian dependence on the magnitude of the Li^6 rf field, H_{16}, for the case where the Li^7 system has been adiabatically demagnetized in the rotating frame; these results show that the Gaussian behavior previously assumed is incorrect. For the case where the Li^7 rf field is of the order of the local field, $W_{CR}(H_{16})$ is asymmetric about Hahn's double resonance (DR) condition, with the larger W_{CR} corresponding to H_{16} less than for the DR condition. The cross-relaxation times at the DR condition are on the order of 0.4 msec. We observe no spin-diffusion bottleneck in a sample of LiF with an isotopic abundance of 0.008% Li^6. Finally, we draw some general conclusions about the application of RFDR to other problems.

I. INTRODUCTION

NUCLEAR double resonance in the rotating frame (RFDR) was first suggested as an ultrahigh-sensitivity NMR technique in 1960 by Hartmann and Hahn.[1] The classic analyses of the method have been given by Hartmann and Hahn[2] (hereafter referred to as HH) using the general density matrix techniques, and by Lurie and Slichter[3] (hereafter referred to as LS) using a thermodynamic treatment. Several groups have used variations of this technique to obtain NMR and NQR spectra of rare isotopes or impurities in solids.[3–14] The work reported here is primarily an experimental study of the RFDR method itself rather than an application of the method to obtain high-sensitivity spectra of a particular solid.

The reader is referred to the excellent descriptions of the general technique given in HH and LS. In Sec. II, we will review these basic ideas principally as a means of introducing our notation.

We consider two nuclear-spin systems with strong resonant rf fields applied to each. The proper way to describe such a system is in a double rotating-frame representation.[2,3] In this representation, each of the two spin species can be made to sense a different "effective field," and thus the effective Zeeman splittings of the two species can be made equal, thereby allowing rapid cross relaxation. This condition of equal effective field splittings is called the double resonance (DR) or Hahn condition.

The standard method of high-sensitivity spectroscopy is then as follows. The rare-species resonance system is modulated in such a way as to pump energy into the rare-spin effective Zeeman levels. This pumped energy

† Work supported under Grant Nos. AFOSR-1065-66 and 69-1749 of the U. S. Air Force Office of Scientific Research.
* N. S. F. Predoctoral Fellow; present address: Department of Physics, University of Illinois, Urbana, Ill.
[1] S. R. Hartmann and E. L. Hahn, Bull. Am. Phys. Soc. **5**, 498 (1960).
[2] S. R. Hartmann and E. L. Hahn, Phys. Rev. **128**, 2042 (1962).
[3] F. M. Lurie and C. P. Slichter, Phys. Rev. **133**, A1108 (1964).
[4] A. G. Redfield, Phys. Rev. **130**, 589 (1963).
[5] R. E. Walstedt, D. A. McArthur, and E. L. Hahn, Phys. Letters **15**, 7 (1965).
[6] Y. Tsutsumi, M. Kunitomo, and T. Hashi, J. Phys. Soc. Japan **20**, 2095 (1965).
[7] R. E. Slusher and E. L. Hahn, Phys. Rev. Letters **12**, 246 (1964).
[8] A. Hartland, Phys. Letters **20**, 567 (1966).
[9] M. Satoh, P. R. Spencer, and C. P. Slichter, J. Phys. Soc. Japan **22**, 666 (1967).
[10] G. T. Mallick and R. T. Schumacher, Phys. Rev. **166**, 350 (1968).
[11] A. Hartland, Proc. Roy. Soc. (London) **A304**, 361 (1968).
[12] R. E. Slusher and E. L. Hahn, Phys. Rev. **166**, 332 (1968).
[13] K. F. Nelson and W. D. Ohlsen, Phys. Rev. **180**, 366 (1969).
[14] E. L. Hahn, *Nuclear Magnetic Resonance and Relaxation in Solids* (North-Holland Publishing Co., Amsterdam, 1965), p. 42.

then leaks into the abundant system via cross relaxation at the DR condition and reduces the order of the abundant system. This reduction of order can easily be detected as a reduction of abundant spin magnetization. In what follows, we will refer to the former system as the pumped system and the latter as the detected system. Thus, the spectrum of the pumped system is normally obtained by observing the loss in order of the detected system for various values of the rf frequency applied to the pumped system.

This paper is primarily concerned with a study of the dynamics of the cross relaxation between the pumped and detected systems. The main results of our work are measurements of the time dependence of the Li^6–Li^7 cross relaxation in LiF for various crystal orientations and for varying degrees of departure from the DR condition.

We should emphasize, however, that when we speak of Li^6–Li^7 cross relaxation for the three-species LiF system, we actually mean the total cross relaxation between the Li^6 Zeeman energy reservoir and all the other parts of the system with which it can cross-relax, i.e., the Li^7 Zeeman reservoir and the total dipole-dipole reservoir. Thus the cross-relaxation rates which we measure cannot be unambiguously attributed to any particular one of the many cross-relaxation routes of this system. Nevertheless, the rates and functional dependences which are obtained by this approach give the essential behavior of the system and are helpful in understanding how RFDR may best be applied to other problems.

In Sec. II, we first define a general system and develop the expression necessary to obtain the cross-relaxation behavior from the measured free-induction-decay data; then we apply this approach to the particular case of Li^6–Li^7 RFDR in LiF. Section III outlines the experimental apparatus and procedure. The experimental data are presented and discussed in Sec. IV. Finally, we give a summary and our conclusions in Sec. V.

II. THEORY

A. General Case

In this section, we will derive an expression relating the loss of spin order of the detected system to the dynamics of the cross relaxation. The type of rf modulation applied to the pumped system in our work is that of periodic 180° phase shifts as used by HH. The on-off modulation used by LS is then a special case of our result.

We consider the system in the double rotating-frame representation. The unitary operator which gives this transformation for H_0 in the z direction is

$$U=\exp(iI_z{}^P\omega_P t+iI_z{}^D\omega_D t)\,, \tag{1}$$

where $I_z{}^P$ and $I_z{}^D$ are the z components of the total spin operators for the pumped and detected spins, respectively, and ω_P and ω_D are the angular frequencies of the rf applied at or near the resonant frequencies, ω_{0P} and ω_{0D}, of the pumped and detected spins, respectively. When $\omega_P=\omega_{0P}$ and $\omega_D=\omega_{0D}$, the secular part of the rotating-frame Hamiltonian following the nth 180° phase shift of the pumped system rf may be written as

$$\mathcal{H}_n=\mathcal{H}_{ZP}(n)+\mathcal{H}_{ZD}+\mathcal{H}_d{}^0+\mathcal{H}_{ZR}+\mathcal{H}_{\text{spin lattice}}\,, \tag{2}$$

where the various terms are defined as follows:

The pumped-spin Zeeman term after the nth 180° phase shift is

$$\mathcal{H}_{ZP}(n)=(-1)^n\gamma_P\hbar I_x{}^P H_{1P}\,, \tag{3}$$

where γ_P is the gyromagnetic ratio of the pumped spins, $I_x{}^P$ is the x component of the total spin operator of the pumped spins, and H_{1P} is the magnitude of the Larmor component of the rf applied at the resonant frequency of the pumped spins.

The detected-spin Zeeman term $\mathcal{H}_{ZD}$ is independent of phase shifts in the pumped-spin rf and thus, for all n, is given by

$$\mathcal{H}_{ZD}=-\gamma_D\hbar I_x{}^D H_{1D}\,, \tag{4}$$

where all terms are the obvious analogs of those defined above for the pumped system.

The secular dipole term is given by

$$\mathcal{H}_d{}^0=\sum_{i<j}(\mathcal{H}_d{}^0)_{ij}\,, \tag{5a}$$

where

$$(\mathcal{H}_d{}^0)_{ij}=\gamma_i\gamma_j\hbar^2\sum_{k,l}(1-3\cos^2\theta_{kl})\times r_{kl}{}^{-3}I_{zk}{}^i I_{zl}{}^j\,,\quad i\neq j \tag{5b}$$

and

$$(\mathcal{H}_d{}^0)_{ii}=\tfrac{1}{4}\gamma_i{}^2\hbar^2\sum_{k,l}(1-3\cos^2\theta_{kl})\times r_{kl}{}^{-3}(3I_{zk}{}^i I_{zl}{}^i-\mathbf{I}_k{}^i\cdot\mathbf{I}_l{}^i)\,. \tag{5c}$$

In the above sums, the indices i and j run over all the different types of spins, e.g., in LiF we consider the P spins (Li^6), the D spins (Li^7), and also the F^{19} spins; the k and l indices refer to different lattice positions for each type of spin.

The fourth term in Eq. (2), $\mathcal{H}_{ZR}$, refers to all other Zeeman terms in the transformed Hamiltonian, e.g., F^{19} Zeeman levels in LiF. Except in very special cases, which we will not consider, these terms correspond to energy-level differences that are much greater than those of the first three terms in $\mathcal{H}_n$; thus these other Zeeman terms will not significantly exchange energy with the first three and, consequently, may be ignored for the purpose of our cross-relaxation calculation. On the other hand, the $\mathcal{H}_d{}^0$ terms corresponding to these other spins can be effectively coupled to the P and D spin systems and, consequently, cannot be neglected in the cross-relaxation process.

Because most of our experiments are performed in a time small compared with the rotating frame T_1, we also make the assumption that spin-lattice relaxation is negligible; we will show in Sec. IV, however, that this theory is easily extended to cases where spin-lattice relaxation is not negligible, provided the characteristic time of the cross relaxation is much shorter than the rotating frame T_1. Thus, in the following analysis, we consider an isolated system whose Hamiltonian is

$$\mathcal{H}_n' = \mathcal{H}_{ZP}(n) + \mathcal{H}_{ZD} + \mathcal{H}_d^0 . \quad (6)$$

At time t following the nth phase shift this system is described by the density matrix $\rho(n,t)$. If there were no more phase shifts after the nth, the system would attain rotating-frame equilibrium at $t=\infty$ and, thus,

$$\rho(n,\infty) = \exp(-\mathcal{H}_n'\beta_n)[\mathrm{Tr}\exp(-\mathcal{H}_n'\beta_n)]^{-1}, \quad (7)$$

where $\mathcal{H}_n'$ is given by Eq. (6) and $(k\beta_n)^{-1}$ is the corresponding rotating-frame equilibrium temperature. The time dependence of the approach to rotating-frame equilibrium is what we mean by the time dependence of the cross relaxation. Thus, if $\Delta E_P(n,t)$ is the difference between the energy of the pumped system at time t after the nth phase shift and the equilibrium energy of the pumped system as described by β_n in Eq. (7), we can define a cross-relaxation function $f(t)$ by

$$f(t) = \Delta E_P(n,t)/\Delta E_P(n,0) , \quad (8)$$

where

$$\Delta E_P(n,t) = E_P(n,t) - E_P(n,\infty) \quad (9)$$

and

$$E_P(n,t) = \mathrm{Tr}[\rho(n,t)\mathcal{H}_{ZP}(n)] . \quad (10)$$

Since we are considering energy transfer only within the isolated system described by $\mathcal{H}_n'$, we also have

$$f(t) = \Delta E_D(n,t)/\Delta E_D(n,0) , \quad (11)$$

where

$$\Delta E_D(n,t) = E_D(n,t) - E_D(n,\infty) \quad (12)$$

and

$$E_D(n,t) = \mathrm{Tr}[\rho(n,t)\mathcal{H}_D] . \quad (13)$$

It is important to realize that we define $\mathcal{H}_D$ to include all the dipolar energies as well as the $\mathcal{H}_{ZD}$ term in Eq. (6), that is,

$$\mathcal{H}_D = \mathcal{H}_{ZD} + \mathcal{H}_d^0 , \quad (14)$$

so that Eqs. (11) and (8) together guarantee that the total energy corresponding to $\mathcal{H}_n'$ is conserved between phase shifts.

Recall that, in order to define $f(t)$, we conceptually interrupted the phase-shift sequence and allowed the system to equilibrate after the nth phase shift. In the actual experiment, of course, the system only evolves for a time τ, the constant time between phase shifts. Thus, we are using the equilibrium condition at $t=\infty$ only to normalize $f(\tau)$; we do not assume equilibrium for all values of τ.

We have also implicitly assumed in the definition of $f(t)$ that f is independent of n. This gives a simple result for the final relation but need not always be the case, for example, if the cross-relaxation process is limited by spin diffusion. However, as we will show later, it is possible to determine experimentally the extent of the n dependence of f and thus to determine whether or not the measured $f(\tau)$ gives the detailed cross-relaxation dynamics as assumed in this theory [$f(\tau)$ independent of n] or some sort of average cross-relaxation behavior [a case where $f(\tau)$ depends on n].

We can now relate the cross-relaxation dynamics to the loss of detected-system order, which is the experimentally measured quantity. We want to obtain first an expression for $E_D(n,\tau)/E_D(n-1,\tau)$, which requires that we relate the energies E_P and E_D just after a 180° phase shift to their values just before the phase shift. Since the phase shifts are applied only to the pumped-spin rf, they affect only the Zeeman energy of these spins. Thus, we have

$$E_D(n,0) = E_D(n-1,\tau) \quad (15)$$

and

$$E_P(n,0) = -\kappa E_P(n-1,\tau) , \quad (16)$$

where $-1<\kappa<1$ and τ is the time between 180° phase shifts. The constant κ is used in Eq. (16) to account for the actual nonideal pumped-system phase shifts. For ideal instantaneous 180° phase shifts, $\kappa=+1$; whereas, in the limit of completely adiabatic 180° phase shifts, $\kappa=-1$, i.e., no net energy is pumped into the system. Thus, κ is a number which relates only to a particular experimental situation and has no universal significance; as will be shown later, κ can be determined experimentally.

The relative heat capacity of the pumped spins ϵ is defined by

$$\epsilon = C_P H_{1P}^2[C_P H_{1P}^2 + C_D(H_{1D}^2 + H_L^2)]^{-1}, \quad (17)$$

where the Curie constant for the pumped spins C_P is

$$C_P = \gamma_P^2\hbar^2 I_P(I_P+1)N_P/3k , \quad (18)$$

in which k is Boltzmann's constant, I_P is the total spin quantum number, and N_P is the number of pumped spins per unit volume; by substituting the subscript D in place of P in Eq. (18) one obtains the expression for C_D. The local field H_L used in Eq. (18) is defined by

$$-C_D H_L^2\beta_n k = \mathrm{Tr}[\rho(n,\infty)\mathcal{H}_d^0] . \quad (19)$$

For systems of interest for RFDR applications $\epsilon \ll 1$, in which case it is possible algebraically to solve[15] the relations given by Eqs. (7)–(16) in the high-temperature limit. To first order in ϵ and for $n \gg 1$, we obtain

$$E_D(n,\tau)/E_D(n-1,\tau) \cong \exp\{-\epsilon(1+\kappa)[1-f(\tau)][1+\kappa f(\tau)]^{-1}\} . \quad (20)$$

[15] D. V. Lang, thesis, University of Wisconsin (unpublished).

We would like an expression for the loss in order of the detected system following a RFDR sequence of N pumped-spin rf 180° phase shifts each separated by a constant time τ. The experimentally measured quantity is the amplitude of the free-induction decay of the detected spins after H_{1D} is pulsed off. This is proportional to $M_D(N,\tau)$, the detected spin magnetization along H_{1D} in the rotating frame after such a RFDR sequence, and we take the ratio $M_D(N,\tau)/M_D(0,\tau)$ to be a measure of the loss of detected spin order.

To relate the above magnetization ratio to the energy ratio in Eq. (20), we note first that, when $N\gg1$,

$$E_D(N,\tau)/E_D(0,\tau)=[E_D(n,\tau)/E_D(n-1,\tau)]^N, \quad (21)$$

and if the detected system is allowed a few tenths of a msec to come to local equilibrium after the Nth phase shift, then we have

$$M_D(N,\tau)/M_D(0,\tau)=E_D(N,\tau)/E_D(0,\tau). \quad (22)$$

Thus, by Eqs. (20)–(22), we obtain our final result

$$M_D(N,\tau)/M_D(0,\tau) \cong\exp\{-N\epsilon(1+\kappa)[1-f(\tau)][1+\kappa f(\tau)]^{-1}\}. \quad (23)$$

This expression reduces to that given in LS if $\kappa=0$ and $f(\tau)=0$, because $\kappa=0$ corresponds to the on-off pumped-spin modulation used by LS, and $f=0$ corresponds to attaining complete equilibrium during each spin-mixing pulse as assumed by LS.

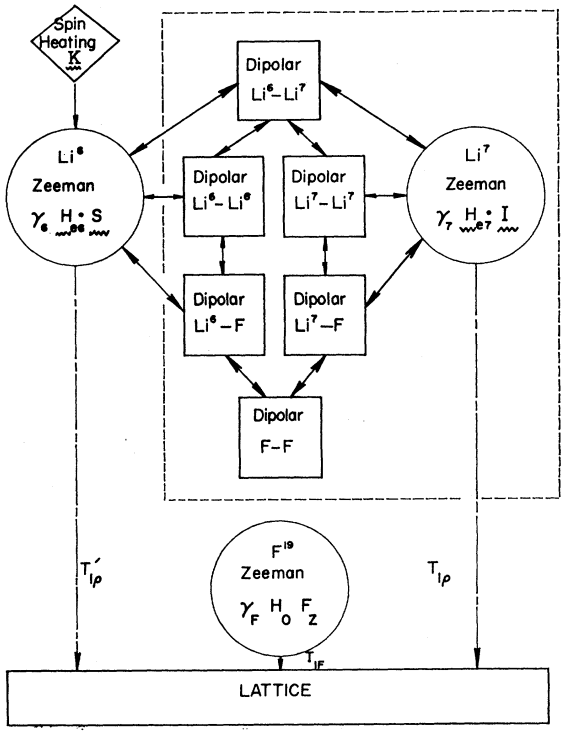

FIG. 1. Schematic representation of rotating-frame sub-Hamiltonian which governs the Li^6–Li^7 cross relaxation.

In order to determine how well Eq. (23) approximates the exact behavior of our model, we have calculated $M_D(N,\tau)$ versus N for different values of ϵ, κ, and f by numerical iteration of Eqs. (7)–(16) with a digital computer. A detailed discussion of the comparison between the exact numerical results and the approximate solution of Eq. (23) is given elsewhere,[15] but the results important to the work reported here can be summarized easily. The discrepancies between the exact model calculations and the approximate expression of Eq. (23) are a maximum for $f(\tau)=0$, corresponding to complete cross relaxation within one heating pulse, and for $\kappa=+1$. For these worst possible conditions, the fractional differences are never greater than ϵ and, as $f(\tau)$ approaches 1, they rapidly approach zero. The situation, however, is even better than these error magnitudes indicate because the incremental slope of the exact solution is at first smaller and then greater than the approximate solution slope. That is, the exact computed solution and the approximate solution given in Eq. (23) always become equal to one another for some value of N and, for ϵ less than about 0.1, this occurs for N within one pulse of the $(1/e)$ points of the curves. Thus, for example, even with $\epsilon=0.1$ and $f(\tau)=0$, the discrepancy between the exact logarithmic slope averaged to the $(1/e)$ point and the approximate slope obtained from Eq. (23) is much less than 1%. Consequently, the errors introduced by using the approximate form given in Eq. (23) are, for the range of ϵ obtained in the experiments reported here, typically much smaller than the noise errors involved in the experimental measurements.

B. Case of LiF

In the experiments reported here, we study the RFDR process in LiF where the pumped spins are Li^6 and the detected spins are Li^7. For this case, the terms in Eq. (6) for $\mathcal{H}_n'$ are given by

$$\mathcal{H}_{ZP}(n)=\mathcal{H}_{Z6}(n)=(-1)^n\gamma_6\hbar I_x{}^6H_{16}, \quad (24)$$

$$\mathcal{H}_{ZD}=\mathcal{H}_{Z7}=-\gamma_7\hbar I_x{}^7H_{17}, \quad (25)$$

and

$$\mathcal{H}_d{}^0=(\mathcal{H}_d{}^0)_{77}+(\mathcal{H}_d{}^0)_{7F}+(\mathcal{H}_d{}^0)_{FF} +(\mathcal{H}_d{}^0)_{76}+(\mathcal{H}_d{}^0)_{F6}+(\mathcal{H}_d{}^0)_{66}, \quad (26)$$

where the terms in $\mathcal{H}_d{}^0$ are given by Eqs. (5a) and (5b) with Li^7, Li^6, and F^{19} denoted by 7, 6, and F, respectively. This system is shown schematically in Fig. 1; the dipole terms of Eq. (26) are represented by squares and the Zeeman terms of Eqs. (24) and (25) are represented by the circles. The detected system consists of those terms enclosed by the dashed lines. Terms that can exchange energy are connected by arrows, indicating possible paths of energy flow. Note that the F Zeeman term is decoupled from the system as explained in Sec. I.

The weak spin-lattice interaction is indicated by the dashed arrows labeled $T_{1\rho}$ and $T_{1\rho}'$.

To calculate H_L from Eq. (19) for LiF, we consider only the first three terms of $\mathcal{H}_d^0$ given in Eq. (26), since the others are negligibly small for the low concentrations of Li^6 used in our samples. Explicit evaluation, as given in LS, of Eq. (19) yields

$$H_L^2=\tfrac{1}{3}\langle\Delta^2H\rangle_{77}+\langle\Delta^2H\rangle_{7F}+\tfrac{1}{3}[\gamma_F^2N_FI_F(I_F+1)/\gamma_7^2N_7I_7(I_7+1)]\langle\Delta^2H\rangle_{FF}, \quad (27)$$

where $\langle\Delta^2H\rangle_{ij}$ is the contribution (in G) of the j spins to the second moment of the i-spin resonance line. Using this definition of H_L, we find that $H_L^2=8.20$, 15.4, and 37.0 G^2 for H_0 along the [111], [110], and [100] directions, respectively, in LiF, these fields referring, as indicated in Eq. (19), to the detected spin Li^7 nuclei, which have $I=\frac{3}{2}$, a gyromagnetic ratio of 1.655 kHz/G, and a natural isotopic abundance of 92.57%. The Li^6 nuclei have a gyromagnetic ratio of 0.627 kHz/G, $I=1$, and a natural isotopic abundance of 7.43%, while F^{19} is 100% abundant with a gyromagnetic ratio of 4.006 kHz/G and spin $\frac{1}{2}$.

III. EXPERIMENTAL APPARATUS AND PROCEDURE

A block diagram of the apparatus is shown in Fig. 2. All data were taken at room temperature with a sample probe of standard crossed-coil geometry very similar to that described in LS. All crystal samples were about 1-cm cubes; the powder sample was hand tamped into a tube of about 1 cm diameter. The optical grade LiF single crystals with normal Li^6 abundance (7.43%) were obtained from the Harshaw Chemical Co. Some of these crystals were irradiated with Cs γ-rays to give an F-center concentration of about 6×10^{16} cm^{-3}. This irradiation lowered the spin-lattice relaxation times to $T_1\approx3$ min in the lab frame and $T_{1\rho}\approx4$ sec in the rotating frame, with the typical orientation dependence of paramagnetic relaxation.[16] The LiF powder was commercial reagent grade with $T_1\approx1.4$ sec and $T_{1\rho}\approx0.8$ sec. A single crystal of LiF with 80-ppm Li^6 was obtained from the Oak Ridge National Laboratory. This sample had $T_1\approx2$ h and $T_{1\rho}\approx4$ min, independent of orientation within about 10%.

The field-regulated Magnion 12″ magnet was set at 8823 G, giving the resonance frequencies of Li^7 and Li^6 at 14.607 and 5.5305 MHz, respectively. The Li^7 electronics system uses the superhetrodyne principle with most amplification and phase-sensitive detection performed at an intermediate frequency of 3.20 MHz. The duration of the H_{16} phase shifts was between 5 and 10 μsec, depending on the tuning of the Li^6 rf transmitter. The magnitudes of H_{17} and H_{16} were measured by observing the respective rf voltages on an oscilloscope; these voltages were calibrated by rotary saturation experiments[17] on the F^{19} resonance in a BaF_2 crystal. This allows us to set H_{16} and H_{17} to within about 3%.

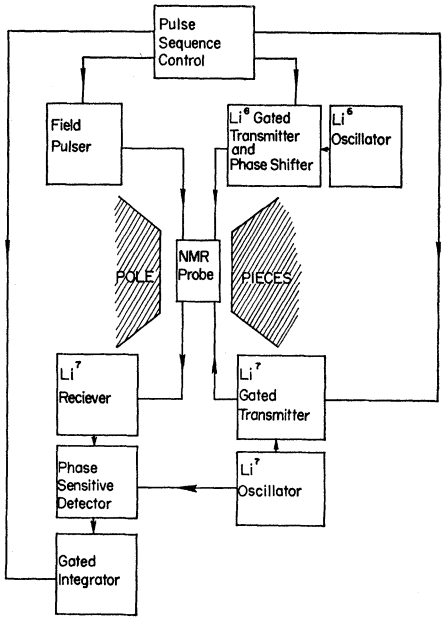

FIG. 2. Block diagram of the RFDR apparatus.

The ordered state of the detected system prior to the RFDR sequence was prepared by polarizing the Li^7 spins for a time on the order of T_1 and then tipping the Li^7 magnetization into the rotating frame along H_{17} by the field-pulse method of LS. This condition is commonly referred to as being spin-locked in the rotating frame. For some data, H_{17} was further reduced nearly to zero after the spin-locking sequence; this is called adiabatic demagnetization in the rotating frame (ADRF). After ADRF, the ordered state is purely dipolar, and the cross relaxation is between $\mathcal{H}_{Z6}(n)$ and $\mathcal{H}_d^0$. In the ADRF case, the order of the detected system is measured following the RFDR sequence by adiabatically increasing H_{17} again to convert part of the dipolar order back into Zeeman order, and then observing the Li^7 magnetization.

In these experiments we must set the Li^7 polarization time between successive RFDR sequences, the delays between the start of the spin-locking field pulse, the H_{17} rf pulse, the H_{16} rf pulse, the boxcar integrator gates, the oscilloscope trigger, and the ADRF sequence (when used). In addition, we must vary independently the shape and length of the spin-locking field pulse, the length of the H_{17} rf pulse, the speed and length of the ADRF sequence, and the H_{16} parameters τ and N. These operations are performed in a simple and direct manner by the pulse sequence control, a hybrid system of Tektronix 160 Series pulse generators driving a programmable unit of our own design made with various digital-logic integrated circuits.

[16] E. R. Andrew, K. M. Swanson, and B. R. Williams, Proc. Phys. Soc. (London) 77, 36 (1961).
[17] J. R. Franz and C. P. Slichter, Phys. Rev. 148, 287 (1966).

The boxcar integrator was used mainly for convenience in recording the single-crystal data. The relatively long T_1's limited data acquisition to about two readings per point, with the exception of the important $M_7(0,\tau)$ points where we took about ten readings. The S/N ratio was no less than 10 in the worst case, so no effort was made to average more data.

IV. EXPERIMENTAL RESULTS

A. Method of Analysis

The main purpose of this work is to determine experimentally the dynamics of the Li^6–Li^7 RFDR cross relaxation in LiF. The raw data which we obtain (FID amplitudes) are proportional to the Li^7 spin-locked magnetization; we use Eq. (23) to extract $f(\tau)$ from these data, for which we have always set $\omega_6=\omega_{06}$ and $\omega_7=\omega_{07}$, as assumed in the derivation of Eq. (23). We also neglected spin-lattice relaxation in deriving Eq. (23); this is certainly valid for cases in which $N\tau \ll T_{1\rho}$. If $N\tau \sim T_{1\rho}$, on the other hand, then the system described by Eq. (6) loses significant energy to the lattice during the RFDR sequence. However, if the cross relaxation proceeds much faster than the spin-lattice relaxation, the system of Eq. (6) loses energy uniformly at a rate determined by the sample average of $T_{1\rho}^{-1}$, and our theory is still valid if we interpret Eq. (23) as giving the fractional magnetization loss due only to RFDR. Thus, we measure $M_7(0,\tau)$ with the same spin-locking time, i.e., length of the H_{17} pulse, as is used for the set of $M_7(N,\tau)$ data which are to be divided by $M_7(0,\tau)$ in Eq. (23).

In general we use the N and τ dependence of a set of Li^7 FID data to obtain a particular $f(\tau)$. Thus we have $f(\tau)$ as a function of H_{16}, H_{17}, orientation, and Li^6 concentration. We have chosen to make H_{16} the prime variable of these four, and thus will give our final results in terms of $f(\tau)$ versus H_{16} for various values of the other three parameters.

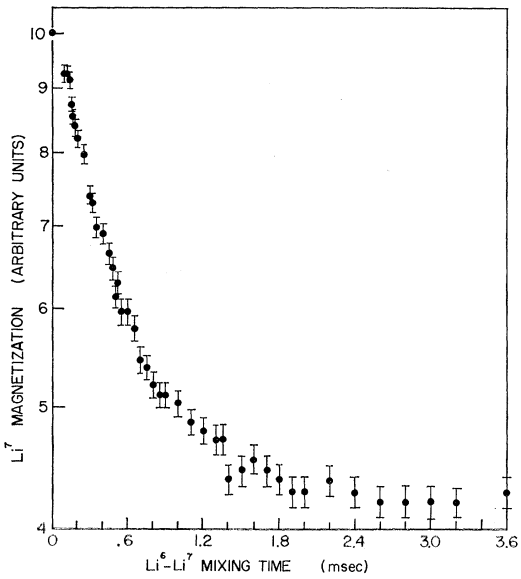

FIG. 3. Log$M_7(N,\tau)$ versus τ; $N=25$, $H_{17}=2.6$ G, $H_{16}=6.9$ G (the DR condition), [111] along H_0, 7.43% Li^6.

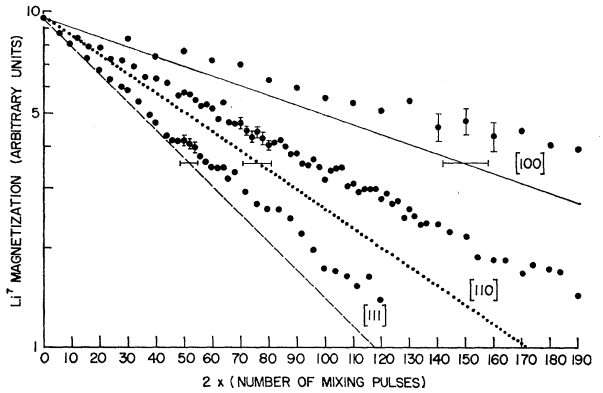

FIG. 4. Log$M_7(N,\tau)$ versus $2N$; $\tau=3.2$ msec, $H_{17}=2.6$ G, $H_{16}=6.9$ G (the DR condition), 7.43% Li^6. The solid, dotted, and dashed lines are calculated from Eq. (23) assuming $\kappa=1$ and $f(\tau)=0$. These lines and the data directly above them correspond to H_0 along [100], [110], and [111], respectively. The error bars on the lines represent the uncertainty in calculating ϵ from Eq. (17).

We now outline how $f(\tau)$ is obtained from a typical set of raw data. Figures 3 and 4 show such data for a crystal of LiF with a natural abundance of Li^6. In Fig. 3 we have plotted $M_7(N_0,\tau)$, i.e., the RDFR Li^7 signal for a fixed N as a function of τ. We first examine the $M_7(N_0,\tau)$ data to determine how large τ must be to ensure complete cross relaxation between phase shifts; this corresponds to being in the flat portion of the curve. According to the definition of $f(\tau)$ in Eq. (8), complete cross relaxation corresponds to $f=0$, so when τ is set to ensure this condition, Eq. (23) becomes simply

$$M_7(N,\tau\to\infty)/M_7(0,\tau)=\exp[-N\epsilon(1+\kappa)]. \quad (28)$$

The data presented in Fig. 4 were taken for long fixed τ, but for variable N, and these $M_7(N,\infty)$ data obey Eq. (28). Thus we can easily obtain $\epsilon(1+\kappa)$ from the slope of log$M_7(N,\infty)$ versus N as in Fig. 4. For our experiments, where the Li^6 isotopic concentrations are known, ϵ can be calculated from Eq. (17), so the $M_7(N,\infty)$ data give an experimental determination of κ. By changing the phase-shift characteristics of the Li^6 transmitter, we can easily cause κ to vary from 0.3 to 0.9. This large departure of κ from 1.0 is due to the strong local fields in LiF, which cause a substantial fraction of the Li^6 magnetization to be lost during the phase shift; by changing the crystal orientation so that H_L goes from 3 G to 6 G, we change κ from 0.8 to 0.5. A determination of κ thus constitutes an apparatus calibration for a particular tuning of the Li^6 rf transmitter and a particular crystal orientation. For our operating conditions, the character of the phase shifts, and thus κ, is independent of N and τ. One can also,

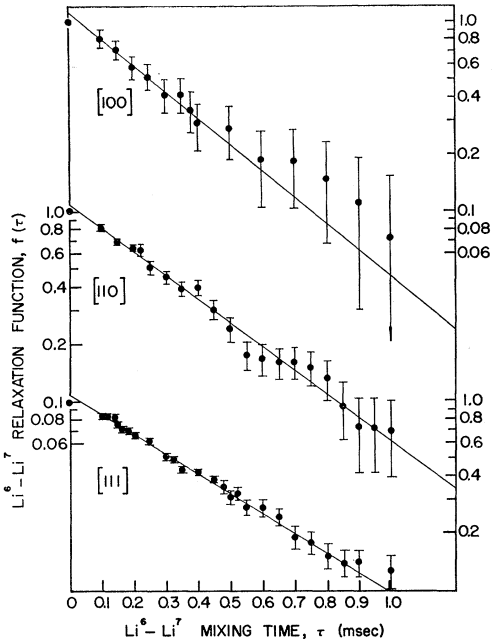

FIG. 5. Log$f(\tau)$ versus τ for H_0 along [100], [110], and [111]; $H_{17}=2.6$ G, $H_{16}=6.9$ G (the DR condition), 7.43% Li^6. The solid lines indicate the exponential dependence of the data.

of course, determine the Li^6 concentration by measuring $\epsilon(1+\kappa)$ in a sample of unknown isotopic abundance, provided κ has been previously determined from a sample of known concentration under the same conditions.

Once κ is known, we can apply Eq. (23) to the $M_7(N_0,\tau)$ data in Fig. 3 to determine $f(\tau)$. Figure 5 shows typical $f(\tau)$ results corresponding to data taken under the same conditions as for Figs. 3 and 4.

At this point, we should examine further the assumption made earlier that $f(\tau)$ is independent of n. The data presented in Fig. 6 show $M_7(N,\tau)$ versus N for values of τ ranging from 0.1 msec to times long enough for essentially complete cross relaxation. For all these values of τ, one sees that, within experimental accuracy, the data exhibit an exponential dependence on N. We take these results to be an indication of the validity of our assumption for the specific systems reported here.

Note, however, that the [111] data in Fig. 4 show very faint, but reproducible, oscillations as a function of N. We have not yet been able to determine whether this is a real, but weak, n dependence of f or some systematic error. At any rate, the effect is weak enough to be neglected for the present purposes of obtaining $f(\tau)$.

B. Behavior of Cross Relaxation

The time dependence of the cross relaxation, as given by $f(\tau)$ in Fig. 5, is well described by an exponential with a "roll-off" at small τ. As experimental parameters are changed, the characteristic times involved in $f(\tau)$

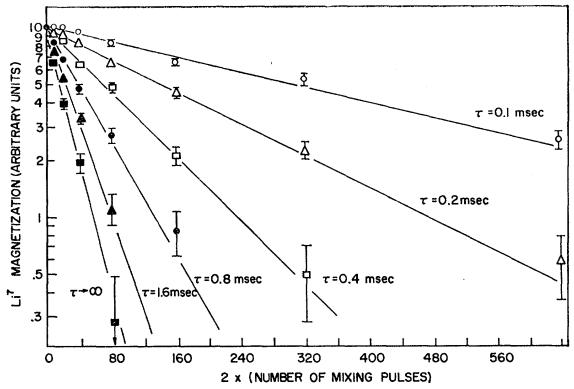

FIG. 6. Log$M_7(N,\tau)$ versus $2N$ for $\tau=0.1$, 0.2, 0.4, 0.8,1 .6, ∞ msec; $H_{17}=3.0$ G, $H_{16}=14.1$ G, H_0 along [110], 7.43% Li^6.

change, but under wide variations of experimental conditions the basically exponential character remains. The small τ roll-off was anticipated theoretically by Redfield,[4] and can be attributed to the cosinusoidal time variation of coherent energy exchange between pumped and detected systems for $\tau<T_2$. The cross relaxation is thus characterized by an initial second-order time variation with the incoherent exponential behavior beginning to emerge after $\tau\simeq T_2$.

Since all measured $f(\tau)$ show the same general exponential behavior, we describe each by its characteristic cross-relaxation time τ_{CR} or cross-relaxation rate, $W_{CR}=(1/\tau_{CR})$, and we obtain W_{CR} from the slope of the best fit to log$f(\tau)$ versus τ as shown in Fig. 5. Note that the W_{CR} values in Fig. 5 vary only from 2.6 to 3.2 $msec^{-1}$, whereas H_L^2 varies from 8.2 to 37 G^2 as the orientation changes from [111], through [110], to [100].

Figure 7 shows W_{CR} versus H_{16}; the lower curve is for the ADRF case ($H_{17}=0$) with [111] parallel to H_0, the orientation of smallest experimental error. Our

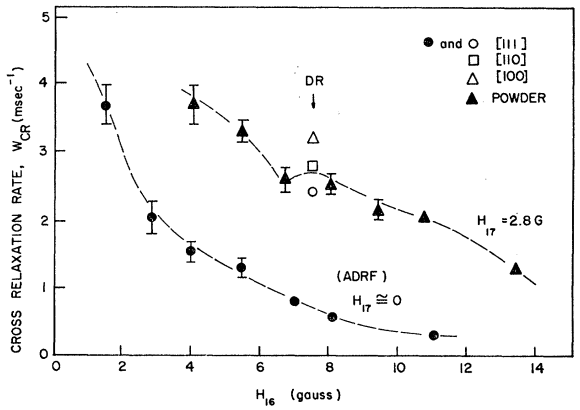

FIG. 7. W_{CR} versus H_{16} for two values of H_{17}. Solid circles: $H_{17}=0$ (ADRF), [111] along H_0, 7.43% Li^6. Solid triangles: $H_{17}=2.8$ G, LiF powder, 7.43% Li^6. Triangle, square, and circle: $H_{17}=2.8$ G, 7.43% Li^6, H_0 along [100], [110], and [111], respectively. The arrow indicates the DR condition for the $H_{17}=2.8$ G data.

measurements for the [110] and [100] orientations show, within experimental accuracy, the same shape as that in Fig. 7 for the [111] case. Just as for the results shown in Fig. 5, the magnitude of W_{CR} increases over the [111] values an average of about 15% and 30% for the [110] and [100] directions, respectively. The relative insensitivity to crystalline orientation appears typical of the LiF system and allows us, at least for semiquantitative purposes, to compare single-crystal and powdered sample results. The upper curve in Fig. 7 shows primarily powdered sample results for the case where $H_{17}=2.8$ G; we observe here that W_{CR} is very asymmetric about the DR condition, with W_{CR} actually growing larger as H_{16} approaches zero. If the only mechanism of cross relaxation were mutual Li^6–Li^7 spin flips along H_{16} and H_{17}, respectively, then one would expect W_{CR} to decrease on the low side as well as the high side of the DR field indicated by the arrow in Fig. 7. In the case where $H_{17}\simeq 0$ (ADRF), we observe that W_{CR} has the long wings characteristic of a Lorentzian or exponential dependence on H_{16}. This behavior is more evident when one plots the ADRF data as τ_{CR} versus H_{16}^2 as is shown in Fig. 8; the good straight line fit for data well into the tails of $W_{CR}(H_{16})$ leaves little doubt about the quasi-Lorentzian shape in contrast to the assumption always made previously[2,3,12] that $W_{CR}(H_{16})$ should be approximately Gaussian.

We have attempted to find semiquantitative interpretations of the behavior of $W_{CR}(H_{16})$, but have been quite unsuccessful. It is clear, however, that the magnitude of W_{CR} near its maximum can be predicted within a factor of 2 by the treatments of HH or LS, whereas the H_{16} dependence does not conform at all to theoretical predictions such as given, for example, in the ADRF case by Slusher and Hahn.[12] Qualitatively, however, certain features of the RFDR behavior suggest that the cross relaxation in LiF is a two-channel process. Referring to the schematic representation in Fig. 1, we note that the Li^6 nuclei communicate with the full detected-system energy reservoir via the Li^6–F dipolar

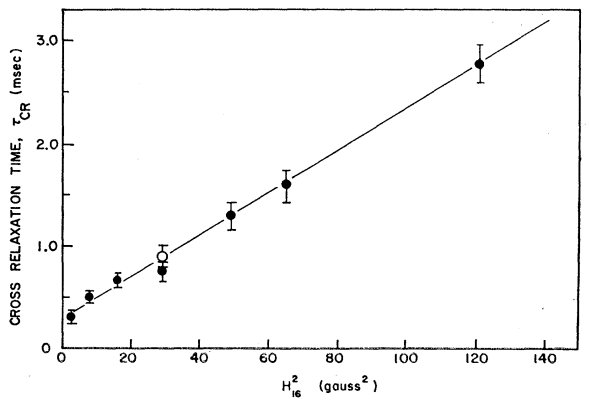

FIG. 8. τ_{CR} versus H_{16}^2; $H_{17}=0$ (ADRF), [111] along H_0, 7.43% Li^6. The circle is for 0.008% Li^6 under the same conditions.

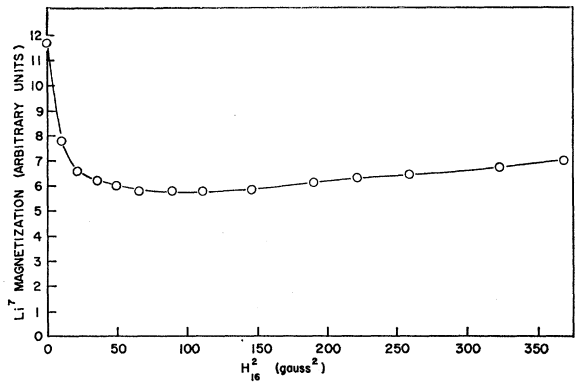

FIG. 9. $M_7(N,\tau)$ versus H_{16}^2; $H_{17}=0$ (ADRF), [111] along H_0, 7.43% Li^6, $N=150$, $\tau=0.2$ msec.

interactions as well as the Li^6–Li^7 interactions. We therefore expect $W_{CR}(H_{16})$ to be the sum of two lines: the first, due to the Li^6–F path, connects to the fluorine dipolar energy reservoir and would be centered at $H_{16}=0$, whereas the second part of W_{CR} is due to the Li^6–Li^7 path and is centered at the DR position. In Fig. 7 for the ADRF case, both contributions are centered at $H_{16}=0$ to produce a relatively narrow shape for W_{CR}, but when $H_{17}=2.8$ G the two components are displaced from one another; we think this effect is the cause of the pronounced asymmetry with respect to the DR field value which was noted above for the case when $H_{17}=2.8$ G. Unfortunately, our present detected-spin transmitter cannot maintain a sufficiently large H_{17} to confirm this speculation by allowing a distinct resolution of the two components of W_{CR}.

Many factors probably contribute to the quasi-Lorentzian shape of W_{CR} versus H_{16} for the ADRF experiments; for example, one can show that higher-order multiple spin-flip processes play a more important role as H_{16} increases, and the relatively large contributions of the F^{19} spins to the Li local fields tends to relate the cross-relaxation line shape to those single-resonance situations where a quasi-Lorentzian line shape can be caused by the presence of a second nuclear species.[18] The presence of the long tails of $W_{CR}(H_{16})$ explains another interesting aspect of RFDR behavior, which is shown for the ADRF case in Fig. 9. These data show a very broad minimum of M_7 as a function of H_{16}, a result first reported for Li metal in LS. To exhibit the source of this behavior, we consider Eq. (23) with the approximation $f(\tau)=\exp(-\tau/\tau_{CR})$ to obtain, for $\tau/\tau_{CR}\ll 1$,

$$M_7(N,\tau)/M_7(0,\tau)\simeq\exp(-T\epsilon/\tau_{CR}), \qquad (29)$$

where $T=N\tau$. Equation (29) serves to illustrate the essential role of ϵ/τ_{CR} as the RFDR M_7 destruction rate; according to the H_{16}^2 dependence of ϵ in Eq. (17)

[18] A. Abragam, *The Principles of Nuclear Magnetism* (Oxford University Press, London, 1961), Chap. IV, Sec. III.

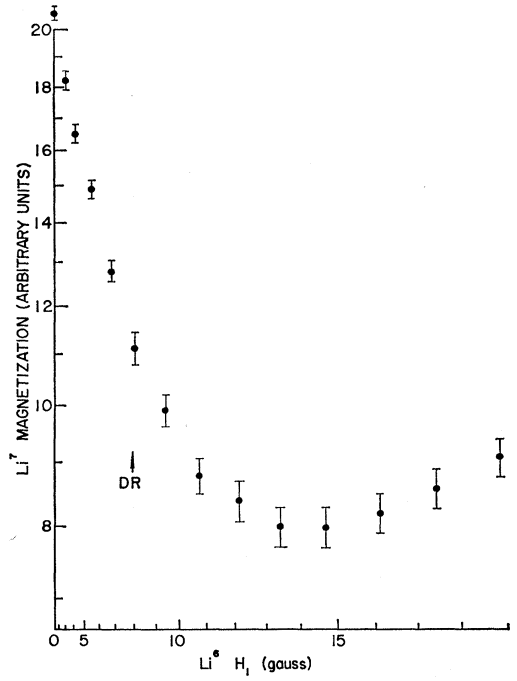

FIG. 10. Log$M_7(N,\tau)$ versus H_{16}^2; $N=40$, $\tau=0.5$ msec, $H_{17}=3.0$ G, [110] along H_0, 7.43% Li^6. The arrow indicates the DR condition for H_{16}.

and τ_{CR} in Fig. 8, ϵ/τ_{CR} should be nearly constant over a wide range of H_{16} to give the broad minimum in M_7 shown in Fig. 9. For the purpose of rough comparison, a Gaussian $W_{CR}(H_{16})$ with a characteristic breadth corresponding to the Li^7 local-field frequencies does fit the data of Fig. 9 reasonably well out to $H_{16}^2=50$ G^2, but for larger H_{16}, M_7 returns rapidly to its initial value, showing less than a 20% destruction at $H_{16}^2=150$ G^2 and less than 3% for $H_{16}^2=300$ G^2. Further analysis of the data of Fig. 9 shows that, for H_{16}^2 greater than 150 G^2, the wings of $W_{CR}(H_{16})$ fall off somewhat more sharply than those of a Lorentzian, but not as sharply as those of an exponential function.

The important parameter for optimizing the RFDR signal is ϵ/τ_{CR} also in experiments where $H_{17}\neq 0$. This is illustrated in Fig. 10, where the increase of ϵ is the dominant H_{16} dependence up to about 15 G, and the Li^7 destruction rate is greatest, in this case, for H_{16} set at about twice the DR condition. Since these experiments show that $W_{CR}(H_{16})$ is not described by a simple line-shape function, at least for $H_{17}\neq 0$, one cannot derive a general expression for the optimum setting of H_{16}; on the other hand, the broad wings which appear to be characteristic of the cross-relaxation line shape tend to make the optimum setting occur over a very wide range of H_{16}.

C. Case of Very Rare Li^6

To determine whether the cross-relaxation characteristics depended on Li^6 concentration, we measured $f(\tau)$ for the Oak Ridge National Laboratory LiF sample which had a specified isotopic abundance of 0.008% Li^6. In this case, we can use RFDR to determine independently the Li^6 concentration in the very dilute Li^6 sample since we know κ from the natural-crystal data. Our measurements of $\epsilon(1+\kappa)$ yield a Li^6 concentration of (0.010 ± 0.001)%; this is in reasonably good agreement with the value specified by ORNL and verifies that any discrepancies between experimental results and theoretical predictions cannot be attributed to gross errors in the assumed Li^6 concentration.

Figure 11 shows $f(\tau)$ for both the 0.008% Li^6 sample and the sample with natural isotopic abundance of 7.43%; all other conditions were the same. One can see from these results that, within the experimental uncertainties, the cross-relaxation dynamics are the same for these two concentrations of pumped spins, and one cannot observe a spin-diffusion bottleneck of the RFDR process even in the very rare Li^6 sample. Using the theoretical treatment of cross-relaxation dynamics proposed by Slusher and Hahn[12] and the measured properties of our LiF samples corresponding to the experimental conditions of Fig. 11, we have calculated the behavior predicted for the 0.008% Li^6 case. The calculated $f(\tau)$ is indicated in Fig. 11 by the dotted curve which exhibits a spin-diffusion-limited initial logarithmic slope somewhat less than half that for the 7.4% natural abundance sample. This diffusion-limited slope continues out until $\tau\simeq 4$ msec before starting slowly to recover toward the nonlimited value; this predicted behavior is well outside the experimental errors of the results presented in Fig. 11.

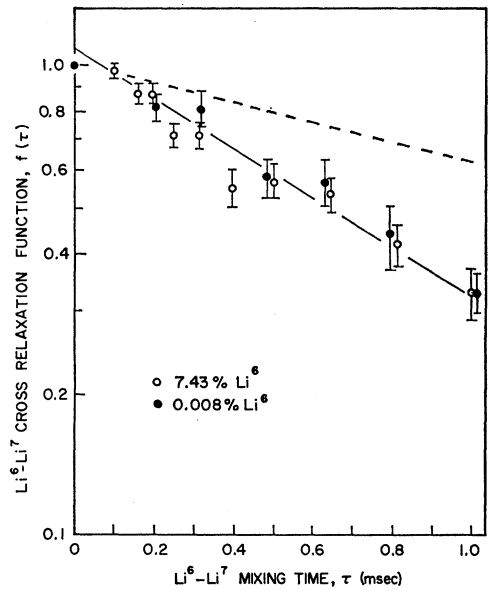

FIG. 11. Log$f(\tau)$ versus τ for 7.43% Li^6 and 0.008% Li^6; $H_{16}=5.4$ G, $H_{17}=0$ (ADRF), [111] along H_0. The dotted curve is calculated from the theory of Slusher and Hahn for 0.008% Li^6 spins in LiF.

We have, consequently, reexamined theoretically the role of spin diffusion in the cross-relaxation process using a different approach than that of Slusher and Hahn. We will present our detailed analysis in a subsequent publication, but our preliminary results show clearly than one should not expect to observe spin-diffusion limitation effects in the system we have studied. It appears that the observable results predicted by the Slusher and Hahn approach arise primarily because the approximations employed give a greatly exaggerated spin heating close to the pumped-spin site as the pumped-spin concentration becomes small.

V. SUMMARY AND CONCLUSIONS

We have observed the dynamics of the cross relaxation between Li^6 and Li^7 in LiF for RFDR. There are four main areas in which we may draw some conclusions.

The first and most obvious conclusion is that the cross relaxation as defined by $f(\tau)$ in Eq. (8) proceeds exponentially for times longer than the order of T_2. For short times, on the order of T_2, we observe a non-exponential roll-off. Such a roll-off ought to be expected and was first predicted by Redfield.[4]

Secondly, we have found that the cross-relaxation rate W_{CR}, for the case in which the Li^7 spins have been adiabatically demagnetized in the rotating frame has a quasi-Lorentzian dependence on H_{16}. This behavior extends well into the tails of a Lorentzian whose half-width is on the order of the local fields in LiF. This quasi-Lorentzian behavior of W_{CR} explains the broad minimum in Li^7 magnetization versus H_{16} for the ADRF case.

Our third set of conclusions concerns the effect on Li^6–Li^7 RFDR of the F^{19} spins in LiF. We have found that such a third species has two main effects. The first is that the dipole-dipole interactions involving the F^{19} spins, as defined in Eq. (26) and shown schematically in Fig. 1, contribute significantly to the heat capacity of the detected system; this must be taken into account in calculating H_L and ϵ. We also find that the F^{19} Zeeman part of the total Hamiltonian plays no role in the Li^6–Li^7 RFDR energy transfer, as ought to be expected. The second effect of the F^{19} spins is to open an additional cross-relaxation path via the Li^6–F dipole-dipole interaction. This two-channel process suggests a qualitative reason for the peculiar changes occurring in $W_{CR}(H_{16})$ when H_{17} is varied as is illustrated in Fig. 7.

Finally, we have looked at a LiF crystal with an isotopic abundance of 0.008% Li^6 and find that the cross-relaxation dynamics are indistinguishable from the behavior of a natural LiF crystal with 7.43% Li^6. Thus there is no detectable spin-diffusion bottleneck at this concentration. We also have found that the RFDR determination of Li^6 concentration for this sample is in good agreement with the concentration determined by other means.

These general conclusions have the following implications for setting optimum experimental conditions in RFDR spectroscopy. First, since $f(\tau)$ is basically exponential, one wants τ as small as possible, but due to the small τ roll-off, one wants τ larger than about T_2. This confirms the criteria proposed by Redfield.[4] Secondly, because of the Lorentzian behavior of $W_{CR}(H_{16})$, the setting of H_{16} is not very critical when the detected system is in the ADRF state, as was first experimentally observed by Lurie and Slichter.[3] The only consideration is that the pumped system H_1 be somewhat larger than the local field. When one is not in the ADRF state, the situation is more complicated and is governed by the dependence of τ_{CR} on H_{1P}; in general, one should expect that the exact DR condition is not necessarily the optimum setting of H_{1P}, as shown, for example, in Fig. 10. For LiF there seems to be a very wide range of H_{16} values which give M_7 destruction close to optimum. Concerning the presence of a third spin species, we observe that RFDR works as expected if one includes the effect of that third species in H_L as shown in Sec. II. In general, a third species decreases the RFDR sensitivity because it tends to decrease ϵ, but this detrimental effect may largely be compensated by the creation of additional cross-relaxation paths which increase W_{CR}. Finally, that we observe no evidence for a spin-diffusion bottleneck in the RFDR cross relaxation, even for our most dilute 0.008% Li^6 sample, implies that the full RFDR sensitivity enhancement for rare-species detection extends to much more dilute rare-species concentrations than previously anticipated.

ACKNOWLEDGMENTS

The authors wish to express thanks to Professor J. R. Cameron for supplying the single-crystal LiF samples and to J. Wagner for performing the irradiation and measuring the F-center concentration of these samples.